Karaica D, et al. Sex-independent expression of Cfex (Slc26a6) in rat pancreas, small intestine, and liver, and male-dominant expression in kidneys
Arh Hig Rada Toksikol 2018;69:286-303

286

Sex-independent expression of chloride/formate exchanger Cfex (Slc26a6) in rat pancreas, small intestine, and liver, and male-dominant expression in kidneys

Dean Karaica[1], Davorka Breljak[1], Jovica Lončar[2], Mila Lovrić[3], Vedran Micek[1],
Ivana Vrhovac Madunić[1], Hrvoje Brzica[1], Carol M. Herak-Kramberger[1], Jana Ivković Dupor[1],
Marija Ljubojević[1], Tvrtko Smital[2], Željka Vogrinc[3], Gerhard Burckhardt[4], Birgitta C. Burckhardt[4],
and Ivan Sabolić[1]

Molecular Toxicology Unit, Institute for Medical Research and Occupational Health[1], Laboratory for Molecular Ecotoxicology, Ruđer Bošković Institute[2], Clinical Institute of Laboratory Diagnosis, University Hospital Center[3], Zagreb, Croatia, Institute for Systemic Physiology and Pathophysiology, University Medical Center Göttingen, Göttingen, Germany[4]

Chloride/formate exchanger (CFEX; SLC26A6) mediates oxalate transport in various mammalian organs. Studies in *Cfex* knockout mice indicated its possible role in development of male-dominant hyperoxaluria and oxalate urolithiasis. Rats provide an important model for studying this pathophysiological condition, but data on Cfex (rCfex) localisation and regulation in their organs are limited. Here we applied the RT-PCR and immunochemical methods to investigate *rCfex* mRNA and protein expression and regulation by sex hormones in the pancreas, small intestine, liver, and kidneys from intact prepubertal and adult as well as gonadectomised adult rats treated with sex hormones. *rCfex* cDNA-transfected HEK293 cells were used to confirm the specificity of the commercial anti-CFEX antibody. Various biochemical parameters were measured in 24-h urine collected in metabolic cages. *rCfex* mRNA and related protein expression varied in all tested organs. Sex-independent expression of the rCfex protein was detected in pancreatic intercalated ducts (apical domain), small intestinal enterocytes (brush-border membrane; duodenum > jejunum > ileum), and hepatocytes (canalicular membrane). In kidneys, the rCfex protein was immunolocalised to the proximal tubule brush-border with segment-specific pattern (S1=S2<S3), and both *rCfex* mRNA and protein expression exhibited male-dominant sex differences driven by stimulatory effects of androgens after puberty. However, urinary oxalate excretion was unrelated to renal rCfex protein expression. While the effect of male-dominant expression of rCfex in renal proximal tubules on urine oxalate excretion remains unknown, its expression in the hepatocyte canalicular membrane may be a pathway of oxalate elimination via bile.

KEY WORDS: *anion exchanger; immunolocalisation; nephrolithiasis; oxaluria; RT-PCR; sex differences; urolithiasis*

Chloride/formate exchanger (CFEX), alias putative anion transporter 1 (PAT-1), is the 6th member of the SLC26 transporter family (SLC26A6 in humans, Slc26a6 in rodents) and is located in the plasma membrane of various cells, where it operates as an exchanger of chloride, bicarbonate, oxalate, formate, sulphate, and hydroxyl ions, involving pairs of these anions (1-4). In several human and animal organs (pancreas, gastrointestinal tract, kidneys) the transporter largely mediates Cl^-/HCO_3^- and/or Cl^-/oxalate exchange, thus contributing to Cl^- (re)absorption and HCO_3^- or oxalate secretion (4-11).

Studies in human organs have revealed abundant expression of *CFEX* mRNA in the kidneys and pancreas, less abundant in the placenta, skeletal muscle, small intestine, heart, and liver, and very low in the lungs, brain, and ovaries (12-15). In mice, *mCfex* mRNA was detected in the heart, stomach, small intestine, liver, kidneys, and skeletal muscle and less in the brain, lungs, colon, and testes (16-18). In rats, *rCfex* mRNA was detected in the uterus (19) and kidneys (10), the pattern in kidneys being cortex > outer medulla > inner medulla. However, tissue localisation of the CFEX/Cfex protein is controversial. In the human pancreas, the protein was immunolocalised to the apical surface of duct cells (13), which supports its proposed role as a luminal Cl^-/HCO_3^- exchanger in pancreatic ducts (4, 8, 9, 20, 21). In human kidneys the transporter was detected in the distal segments of proximal tubules and in several more distal nephron segments (12). In another study, the protein was immunolocalised to both apical and basolateral surfaces of non-specified renal tubules (13), which is at odds with the findings in rodent

Correspondence to: Ivan Sabolić, MD, PhD, Molecular Toxicology Unit, Institute for Medical Research and Occupational Health, Ksaverska cesta 2, 10000 Zagreb, Croatia, E-mail: *sabolic@imi.hr*

kidneys. In mice, the mCfex protein was localised to the brush-border membrane (BBM) of cortical proximal tubules (11, 16), apical membrane of villous and crypt cells in duodenum (18), glandular cells in the stomach (22), and the membranes of atrial and ventricular myocytes in the heart (23, 24). These localisations are in accordance with mCfex-mediated anion exchange demonstrated in functional studies (5–7, 18, 22–29). In rats, the functional rCfex protein was demonstrated in microperfusion experiments, and immunolocalised to the proximal tubule BBM (10).

Most characteristics of this transporter have been obtained from studying orthologues in human and mouse organs; much less is known about other species, including rats [reviewed in (1)]. Human CFEX (759 amino acid residues) has been described as a variably glycosylated protein with an apparent M_r ranging from ~84 kDa to ~200 kDa (14, 15, 30). The mouse protein (mCfex; 758 amino acid residues; M_r ~83 kDa) is 79 % homologous with the human (16). In various mCfex-transfected cell lines and in mouse organs (pancreas, intestine, kidneys, and heart) the M_r of mCfex protein ranges between ~80 kDa and ~120 kDa (5, 16, 18, 23, 29–32). One study reported M_r of ~90 kDa for a rat Cfex protein (rCfex; 758 amino acid residues; M_r~83 kDa) in isolated renal BBM (10).

Based on the studies in knockout mice, two oxalate transporters, sulphate anion transporter 1 (Sat-1/Slc26a1) and Cfex have been proposed to play a role in the development of hyperoxalaemia, hyperoxaluria, and oxalate urolithiasis, a disease which in men occurs 2-3 times more often than in women (2, 25, 33–36). Possible contribution of Sat-1 in generating male-dominant hyperoxaluria and nephrolithiasis was further suggested by a finding of strong, androgen hormone-driven sex differences (males > females) in the expression of Sat-1 protein and associated oxalate transport in the hepatocyte sinusoidal membrane (liver being the major oxalate-producing organ) and renal proximal tubule basolateral membrane (kidney being the oxalate-secreting organ) (37). However, later studies in mice (38) and rats (39, 40) could not confirm a significant contribution of hepatic and renal Sat-1 in this male-dominant pathophysiological condition. Other studies using mCfex knockout mice have shown that the Cfex transporter has a major constitutive role in oxalate secretion across the small intestine, which limits the existing paracellular net intestinal absorption of dietary oxalate (25, 28, 32). Apart from exhibiting a greatly reduced secretory flux, which led to hyperoxalaemia and hyperoxaluria, Cfex-deficient mice exhibited strong sex-related oxalate urolithiasis, with 3-4 times higher prevalence in males than in females (25, 34). However, the cause of this phenomenon has not been identified. We do not know if there are sex differences in CFEX/Cfex mRNA and/or protein expression in major oxalate-handling organs (intestine, liver, and kidneys) of adult humans and animals and if these sex differences affect the oxalate secretory function of these organs in health and disease. In view of these unknowns, the present study was performed in rats, aiming to: a) detect rCfex mRNA expression in pancreas, gastrointestinal tract, kidneys, and liver, b) immunolocalise in detail the rCfex protein in these organs using an antibody with tested specificity, c) detect possible sex-related differences in the expression of rCfex in these organs at mRNA and protein levels, and d) to link the renal expression of rCfex with urine excretion of oxalate in male and female rats.

MATERIALS AND METHODS

Animals

In this study, we used prepubertal (three weeks old; N=4) and adult (12-13 weeks old; N=3–10 per experimental group) male and female Wistar rats bred at the Institute of Medical Research and Occupational Health (IMROH) in Zagreb, Croatia. The animals were handled in accordance with the Directive 2010/63/EU on the protection of animals used for scientific purposes and their use was approved by the Ethics Committee of IMROH [Approval No. 100-21/14-7 of 11-06-2014] and by the Ministry of Agriculture, Zagreb [Approval No. 525-10/0255-15-4 of 08-09-2015]. Before and during experiments, the animals received standard pelleted food (4RF21, Mucedola, Italy) and had free access to tap water.

Gonadectomy and sex hormone treatment

Prepubertal rats were not treated and were sacrificed at three weeks of age. Adult rats were either untreated, sham-operated, or gonadectomised and were sacrificed at 12-13 weeks of age. Gonadectomy was performed on six-week old males by the scrotal route (castration) and females (ovariectomy) by the dorsal (lumbal) approach under general intraperitoneal anaesthesia (ketamine hydrochloride, 80 mg kg^{-1} bm + xylazine hydrochloride, 12 mg kg^{-1} bm). Sham-operated animals underwent the same procedure, but without removing gonads. Gonadectomised and sham-operated rats were left to recover for six to seven weeks before sacrifice. Four castrated animals in each treated group received subcutaneous injections of either sunflower oil (vehicle) or sex hormones (testosterone enanthate, oestradiol dipropionate, or progesterone; each (2.5 mg kg^{-1} bm per day for 14 days) dissolved in the vehicle. Four control animals received an equivalent amount of oil [0.5 mL kg^{-1} bm per day for 14 days].

Sacrificed animals were harvested for kidneys, liver, pancreas, and various intestinal segments (duodenum, jejunum, ileum, cecum, and colon), which were then used for reverse transcription polymerase chain reaction (RT-PCR) and immunochemical studies as described below.

Karaica D, et al. Sex-independent expression of Cfex (Slc26a6) in rat pancreas, small intestine, and liver, and male-dominant expression in kidneys
Arh Hig Rada Toksikol 2018;69:286-303

288

Determination of urine parameters

Three days before sacrifice, each rat was placed in its own metabolic cage with free access to water but without food. Over the next 24 h their urine was collected and its volume measured together with their body mass. Urine was centrifuged at 2,500 *g* for 15 min to remove debris, and creatinine, osmolality, citrate, calcium, and oxalate were determined in the supernatant as described elsewhere (40).

Antibodies

An affinity purified goat polyclonal antibody for C-terminal peptide of the human CFEX [CFEX-Ab, #sc-26728 (C-17)] with possible cross-reactivity to rat and mouse Cfex proteins, the related immunising peptide (#sc-26728 P), and monoclonal antibody against Na^+/K^+-ATPase α1-subunit (Na^+/K^+-ATPase-Ab, #sc-48345) were purchased from Santa Cruz Biotechnology, Inc. (Santa Cruz, CA, USA). Monoclonal pan-actin antibody (actin-Ab) was purchased from Millipore (Tamecula, CA, USA, #MAB1501R). The mouse monoclonal 6xHis antibody (6xHis-Ab) was purchased from Clontech Labs/TakaRa Bio USA, Inc. (Mountain View, CA, USA, #631212). Secondary antibodies were purchased from Jackson ImmunoResearch (West Grove, PA, USA) or Kirkegaard and Perry (Gaithersburg, MD, USA) and included the CY3-labelled donkey anti-goat IgG (DAG-CY3), FITC-labelled goat anti-mouse IgG (GAM-FITC), and alkaline phosphatase-labelled rabbit anti-goat (RAG-AP) and goat anti-mouse IgG (GAM-AP).

Chemicals and other material

Anaesthetics ketamine hydrochloride and xylazine hydrochloride (Narketan and Xylapan, respectively) were purchased from Chassot (Bern, Switzerland), sunflower oil solutions of testosterone enanthate, oestradiol dipropionate, and progesterone from RotexMedica (Trittau, Germany) and Galenika (Belgrade, Serbia), the Immobilon membrane from Millipore (Bedford, MA, USA), the markers of protein molecular mass from Fermentas Int. (Ontario, Canada), and Superfrost® Plus microscope slides from Thermo Scientific (Braunschweig, Germany). Other chemicals and reagents used in this study were of analytical grade and purchased from Sigma (St. Louis, MO, USA) or Fisher Scientific (Pittsburgh, PA, USA).

RNA isolation, cDNA synthesis, end-point and real-time RT-PCR

The abdomen of anaesthetised rats was opened, their large blood vessels cut and exsanguinated under a stream of cold water, organs removed, shortly blotted on a filter paper, and ~1 mm thick tissue slices of each kidney (middle transversal slice), liver, pancreas, and intestinal segments (duodenum, jejunum, ileum, cecum, and colon) cut off, and immediately immersed in a RNAlater solution (Sigma, St. Louis, MO, USA). Total RNA from these tissues was extracted using Trizol (Invitrogen, Karlsruhe, Germany) and subsequently purified using the RNeasy Mini Kit (Qiagen, Venlo, The Netherlands) respecting the manufacturer's instructions. RNA concentration and purity were estimated spectrophotometrically (BioSpec Nano, Shimadzu, Japan), and the integrity of RNAs was verified under ultraviolet light after agarose gel electrophoresis and ethidium bromide staining. Isolated RNA was stored at -70 °C until further use. First strand cDNA synthesis was performed using the High-Capacity cDNA RT Kit (Applied Biosystems, Foster City, CA, USA) following the manufacturer's instructions. cDNA was stored at -20 °C until further use.

The end-point PCR was performed on a 25 µL total volume sample with 100 ng of the first-strand cDNA template, 0.4 µmol L^{-1} of specific primers, 0.2 mmol L^{-1} of dNTP mixture (Applied Biosystems, USA), 1x AmpliTaq® DNA polymerase buffer (Applied Biosystems), 0.025 U µL^{-1} of AmpliTaq® DNA polymerase (Applied Biosystems), and 14.9 µL nuclease-free water. The primers for *rCfex*, *rβ-actin*, and *rHprt1* genes were custom-designed with a Primer 3 freeware (41, 42), and synthesised and purchased from Invitrogen (Carlsbad, California, USA). Intron over-spanning primers were used to avoid amplification of genomic DNA. The exact sequence of these primers and their predicted size are listed in Table 1.

Reaction conditions during PCR were as follows: initial DNA denaturation at 94 °C for 3 min, DNA denaturation at 95 °C for 30 sec, annealing at 57 °C for 30 sec, and elongation at 72 °C for 45 sec. PCR products were separated with electrophoresis in 1.5 % agarose gel stained with ethidium bromide and visualised under ultraviolet light. Non-template control reactions, where cDNA was substituted with nuclease-free water, did not result in detectable products indicating contamination-free PCR reactions (data not shown). cDNA input variations were controlled in different tissues with two housekeeping genes (*rβ-actin* and *rHprt1*). The number of PCR cycles within the exponential phase of the PCR reaction was 30 cycles for *rCfex* in the kidney, liver, and pancreas, 23 cycles for *rCfex* in the intestinal segments, 25 cycles for *rβ-actin* in the kidney and liver, 30 cycles for *rHprt1* in the pancreas, and 27 cycles for *rHprt1* in the intestinal segments.

Quantitative real-time RT-PCR (qRT-PCR) of independent renal RNA isolated from four intact rats of each sex was performed on a 25 µL total volume sample with 100 ng of the first-strand cDNA template, 12.5 µL of 2x TaqMan® Universal PCR Master Mix, and 1.25 µL of 20x TaqMan® Gene Expression Assays mix (all from Applied Biosystems). Primers and probes were designed by Applied Biosystems and supplied as a TaqMan® Gene Expression Assay mix containing a 20x mix of unlabelled PCR forward and reverse primers and a TaqMan® MGB probe. Assay IDs for the rat genes were Rn01445892_m1 (*rCfex*) and Rn00667869_m1 (*rβ-actin*). mRNA was

Table 1 *Primer sequences used for end-point RT-PCR*

Gene	Forward (f) / reverse (r) primers (5'→3')	Accession No. Gene Bank	Location	PCR product size (bp)
rCfex	f:GGCTCTTGGGTGACCTGTTA r:AGGTGACCACAAAACCGAAG	NM_001143817.1	302-321 639-658	357
rβ-actin	f:GTCGTACCACTGGCATTGTG r:AGGAAGGAAGGCTGGAAGAG	NM_031144.3	515-534 859-878	364
rHprt1	f:TGCTCGAGATGTCATGAAGG r:AGAGGTCCTTTTCACCAGCA	NM_012583.2	213-232 554-573	361

quantified with TaqMan® Assays (Applied Biosystems) according to the manufacturer's instructions. Amplification and detection were performed using the 7500 RT-PCR System (Applied Biosystems). Thermal cycling conditions were 50 °C for 2 min and 95 °C for 10 min, followed by 40 two-step cycles of denaturation (95 °C for 15 sec) and annealing/extension (60 °C for 1 min). NTC reactions were included in each run to check for possible contamination. The housekeeping gene *rβ-actin* was quantified for endogenous control, and the results were normalised to these values. mRNA expression was quantified with the comparative CT method using the Relative Quantification Study Software supplied by Applied Biosystems (43). Each reaction was performed in duplicate.

Cloning and expression of rCfex in HEK293 cells

The *rCfex* gene coding sequence (GeneBank accession number NP_001137289.1) was amplified from the previously synthesised rat kidney cDNA using forward and reverse primer pairs (Table 1) with Phusion High-Fidelity DNA polymerase (Finnzymes, Vantaa, Finland). The amplicon was cloned into pJET 1.2 vector (ThermoFisher Scientific, Waltham, MA, USA) following the previously described procedure (44). Recombinant plasmid carrying the cloned *rCfex* sequence was purified from two transformed (PCR-screened) competent bacterial DH5α cells (clones) (ThermoFisher Scientific) using the plasmid isolation kit QIAprep Spin Miniprep Kit (Qiagen). The *rCfex* gene sequence was verified by sequencing of both purified plasmids on an ABI PRISM® 3100-Avant Genetic analyser with the primers listed in Table 2. Using the introduced sites for *NheI*, *EcoRI*, and *ApaI*, and restriction enzyme digestion, it was possible to subclone *rCfex* cDNA from the pJET 1.2 multiple cloning site into pcDNA3.1/

HisC (Invitrogen) expression vector with and without the polyHis tag (Invitrogen). Both pcDNA vectors were used in parallel to transiently transfect HEK293 cells using the PEI (polyethyleneimine) reagent method (45). An additional HEK293 cell culture was used as negative control, which underwent the same transfection procedure, except that the plasmid did not contain the *rCfex* gene sequence (vector-transfected cells). For immunocytochemical studies the cells were seeded 48 h before transfection in coverslip 24-well plates at cell density of 1.85×10^5 cells per mL. Transfection efficiency was evaluated 24 h after transfection on a separate HEK293 cell culture with pcDNA3.1/His/LacZ plasmid following the LacZ staining protocol (46).

Immunocytochemistry

When transfection efficiency exceeded 70 % (24 h after transfection), *rCfex*-transfected and vector-transfected HEK293 cells on coverslips were fixed in 4 % *p*-formaldehyde (PFA) for 30 min, extensively rinsed in PBS, and then stored in PBS at 4 °C until further use. Removed tissue pieces (kidney, liver, pancreas, duodenum, jejunum, ileum, cecum, and colon) were fixed overnight in 4 % PFA, extensively rinsed in PBS, and stored in PBS (+0.02 % NaN_3) at 4 °C. When needed, they were infiltrated with 30 % sucrose (in PBS) overnight, frozen at –25 °C, cut into 4-μm thick cryosections (cryostat Leica CM 1850, Leica Instruments, Nussloch, Germany), and placed on Superfrost® Plus microscope slides (Fischer Scientific).

Optimal steps for immunostaining with fixed HEK293 cells have been described in detail earlier (37, 40) and included microwave heating in citrate buffer (pH 6), treatment with Triton X-100 containing buffers, incubation in primary CFEX-Ab, Na^+/K^+-ATPase-Ab or 6xHis-Ab (each diluted in PBS, 1:100) at 4 °C overnight, rinsing in

Table 2 *Forward (f) and reverse (r) primer sequences used for* rCfex *gene cloning and sequencing*

Primer position	Primer sequence (5'→3')	Restriction enzyme sites
f	*TTA*G^CTAGC*G*^A̲A̲T̲T̲C̲ATGGGACTGCCTGATGGGT	*NheI*, *E̲c̲o̲R̲I̲*
r	*TTA*GGGCC^CT*C*^T̲C̲G̲A̲GTCAGAGTTTGGTGGCCAAAAC	*ApaI*, *X̲h̲o̲I̲*
f 695	TCAAGTATGTGTTTGGCATCAA	/
r 800	TTGCTGTGACCACGGTGC	/
f 1400	TCTGGAAGGCAAATCGAGT	/
r 1500	GAAGACTATGGAGACTGCC	/

The underlined parts of primer sequences were introduced for digestion with specific restriction enzymes

Karaica D, et al. Sex-independent expression of Cfex (Slc26a6) in rat pancreas, small intestine, and liver, and male-dominant expression in kidneys
Arh Hig Rada Toksikol 2018;69:286-303

290

Triton-X-100 containing buffers, incubation in secondary antibodies DAG-CY3 or GAM-FITC at room temperature for 1 h, and extensive rinsing in PBS between all incubations. In some experiments, CFEX-Ab was pre-incubated with its immunising peptide (0.5 mg mL^{-1}) at room temperature for 4 h before immunocytochemistry. In double staining experiments (CFEX-Ab + Na$^+$/K$^+$-ATPase-Ab), tissue cryosections were first incubated with CFEX-Ab overnight, then with DAG-CY3 for 1 h, then with Na$^+$/K$^+$-ATPase-Ab overnight and GAM-FITC for 1 h, applying all other steps as described above. The samples were finally overlaid with fluorescence fading retardant Vectashield (Vector Laboratories, Burlingame, CA), closed with a coverslip, and the resulting immunostaining was examined with an Opton III RS fluorescence microscope (Opton Feintechnik, Oberkochen, Germany). Images were taken with the computer-guided Spot RT slider digital camera and software (Diagnostic Instruments, Sterling Heights, MI, USA). All images were taken using the identical microscope and camera settings and imported into Adobe Photoshop 6.0 (Adobe Systems, San Jose, CA, USA) for processing, assembling, and labelling.

Pixel intensity of CY3 fluorescence was measured in the original images with Image-J software, version 1.46r (NIH, Bethesda, MD, USA). In one cryosection of each organ stained with CFEX-Ab, three to four representative images were captured using the 25x magnification objective. In each image, six to ten randomly-chosen regions of interest (ROI) of the staining-positive membranes were encircled. Fluorescence intensity in ROI was measured, averaged, and subtracted for background fluorescence intensity of non-stained cytoplasm. The average value of all measurements in respective cryosections was used as one datum in further calculations.

Western blotting

The removed kidneys were decapsulated and used *in toto*, or the tissue was manually dissected into cortex and outer stripe and processed further as separate tissue pools. The main liver lobe and the pancreas were used *in toto*. The intestinal segments (duodenum, jejunum, ileum, cecum, and colon) were separated, and their mucosa scraped and processed further. Tissue samples were homogenised, and total cell membranes (TCM; pellet between 6,000 *g* and 150,000 *g*) were isolated from each homogenate by differential centrifugation, as previously described in detail elsewhere (37). Proteins were measured with the Bradford assay (47).

For PAGE, isolated TCM were prepared in reducing conditions (with 5 % β-mercaptoethanol) at 65 °C for 15 min, their proteins (80 μg lane^{-1}) separated through 10 % SDS-PAGE mini gels, and wet-transferred by electrophoresis to an Immobilon membrane (Millipore, Bedford, MA, USA) as described in detail elsewhere (37). The Immobilon membrane was then incubated in the buffer containing CFEX-Ab (1:250) or actin-Ab (1:1000) at 4 °C overnight, rinsed, incubated in RAG-AP (1:500) or GAM-AP (1:1000) at room temperature for 1 hour, and rinsed again. Protein bands were visualised at pH 9 via alkaline phosphatase activity-mediated reaction using the BCP/NBT method (37). To verify the specificity of CFEX-Ab for its immunising peptide, the antibody was pre-incubated with the peptide (0.5 mg mL^{-1}) at room temperature for 4 h and used in the blotting assay. Labelled protein bands were evaluated by densitometry using Image-J software. The broadest protein band of rCfex or actin was encircled, an equal area was then applied to other related bands on the same membrane, and the area density of each band was expressed in arbitrary units, relative to the broadest band density (=1 unit).

Statistical analysis

Immunochemical data represent the findings for three to four animals from each experimental group. RT-PCR was done with cDNA obtained from independent RNA preparations from individual organs of three to four animals from each experimental group. Data shown as mean±standard deviation (SD) were statistically analysed with either Student's *t*-test or ANOVA/Duncan test at 5 % level of significance using Statistica 10 (StatSoft, Tulsa, OK, USA).

RESULTS

Expression of rCfex mRNA in rat organs

Figure 1 shows that the expression of *rCfex* mRNA measured at 30 PCR cycles varied between the pancreatic, renal, and liver tissues. In the intestine, its expression was segment-dependent. Measured at 23 PCR cycles, the expression pattern was as follows: duodenum > jejunum > ileum. In the stomach (not shown), cecum, and colon it was negligible, and barely increased at 30 PCR cycles (data not shown).

Immunochemical characterisation of CFEX-Ab in rCfex-transfected HEK293 cells

In preliminary immunocytochemical experiments, we have tested the CFEX-Ab in cryosections and paraffin sections of human, mouse, and rat kidneys and liver by applying different antigen-unmasking techniques (48), and found immunoreactivity only in rat organs (data not shown). To verify the specificity and efficiency of this antibody in detecting the rCfex protein, CFEX-Ab was tested in vector- and *rCfex*-transfected HEK293 cells. Figure 2A shows that CFEX-Ab stained the plasma membrane of *rCfex*-transfected, but not of vector-transfected cells, whereas Na$^+$/K$^+$-ATPase-Ab stained the plasma membrane of both kinds of transfected cells. In addition, *rCfex*-transfected cells were not stained when we used CFEX-Ab pre-incubated with its immunising peptide (Figure 2B). These findings suggest that CFEX-Ab is specific for the rCfex protein in
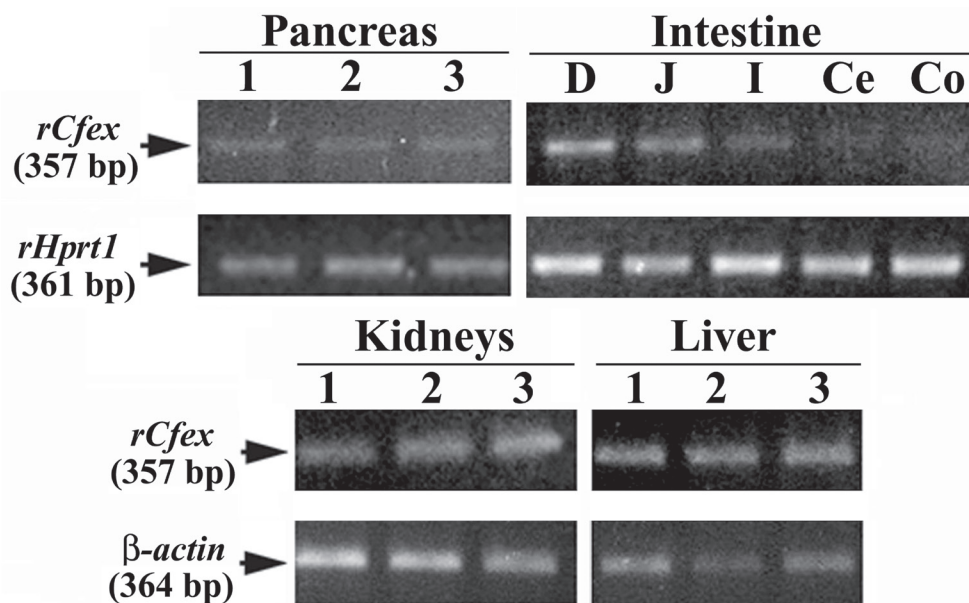
Figure 1 rCfex *mRNA expression in rat organs as determined by end-point RT-PCR. Housekeeping genes* rHprt1 *and* β-actin *were used as loading controls. RNA was isolated from the pancreas, kidneys, and liver of three male rats. For each intestinal segment one male rat was used, but representative for similar findings in three animals. D – duodenum; J – jejunum; I – ileum; Ce – cecum; Co – colon*

immunocytochemical analysis. In order to obtain a visible rCfex-related protein band for SDS-PAGE and Western blotting, we isolated the plasma membranes from the *rCfex*-transfected and vector-transfected cells and incubated them with or without reducing agent (5 % β-mercaptoethanol) at different temperatures (37 °C for 30 min, 65 °C for 15 min, 95 °C for 5 min). However, for unknown reason, we obtained none (data not shown), as opposed to rat tissues.

Expression of the rCfex protein in pancreas

In the Western blots of the TCM isolated from the pancreas of male rats, CFEX-Ab labelled a single protein band of ~120 kDa (Figure 3A, -P), which was absent when the antibody was blocked with the immunising peptide (+P). Similarly, CFEX-Ab stained the luminal domain of acini (Fig. 3B, -P, arrowhead) in tissue cryosections, but there was no staining when the antibody was blocked with the immunising peptide (+P) (Figure 3B). In double staining experiments (Figures 3C, X, Y, and W), CFEX-Ab stained the luminal domain of acini in red-yellow (arrows), whereas Na$^+$/K$^+$-ATPase-Ab stained the cell basolateral membrane in green (arrowheads). CFEX-Ab also stained the luminal membrane of initial (intercalated) ducts (Y, double arrowhead), but not the Langerhans' islet cells (W, LI) and large pancreatic ducts (W, asterisk). Because of the low image resolution we could not discern if the luminal staining in the acini was present only in the membranes of initial (intercalated) ducts or also in the luminal membrane of acinar cells. However, numerous discrete red-stained organelles inside the acinar cells (Figures 3C, Y, and inset in Figure 3F, Male) indicate that rCfex may also be present inside the acinar cells. In the Western blots of TCM with CFEX-Ab and actin-Ab (Figure 3D) and in the densitometric

evaluation of the protein bands (Figure 3E) the related band density of each protein was similar in both sexes. This result was confirmed in tissue cryosections from male and female organs, where CFEX-Ab-related immunostaining in pancreatic ducts was similar in both sexes (Figure 3F).

Expression of the rCfex protein in intestine

In the Western blots of TCM isolated from duodenal mucosa, CFEX-Ab labelled a protein band of ~120 kDa (Figure 4A, -P) but the staining was absent when the antibody was blocked with the immunising peptide (+P). The same was true for the cryosections of the duodenal tissue; CFEX-Ab strongly stained the BBM of enterocytes (Figure 4B, -P), but the staining was absent when the immunising peptide-blocked antibody was used (+P). In Western blots of TCM from various intestinal segments, CFEX-Ab and actin-Ab labelled the rCfex protein band in the membranes from the duodenum and jejunum (duodenum > jejunum), but not in ileum, cecum, and colon (Figures 4C and D). Accordingly, in tissue cryosections the rCfex protein was immunolocalised to the BBM of enterocytes in the duodenum and jejunum (duodenum > jejunum) but not in the ileum, cecum, and colon (Figures 4E and F). The staining intensity in the duodenal villi increased about six times towards the tip compared to the basal domain (Figures 4G and H). The staining distribution and intensity was similar between males and females (data not shown).

Segmental, zonal, and sex differences in kidney rCfex *expression*

In Western blots of the TCM from the whole male kidneys, CFEX-Ab labelled a single protein band of

Karaica D, et al. Sex-independent expression of Cfex (Slc26a6) in rat pancreas, small intestine, and liver, and male-dominant expression in kidneys
Arh Hig Rada Toksikol 2018;69:286-303

292
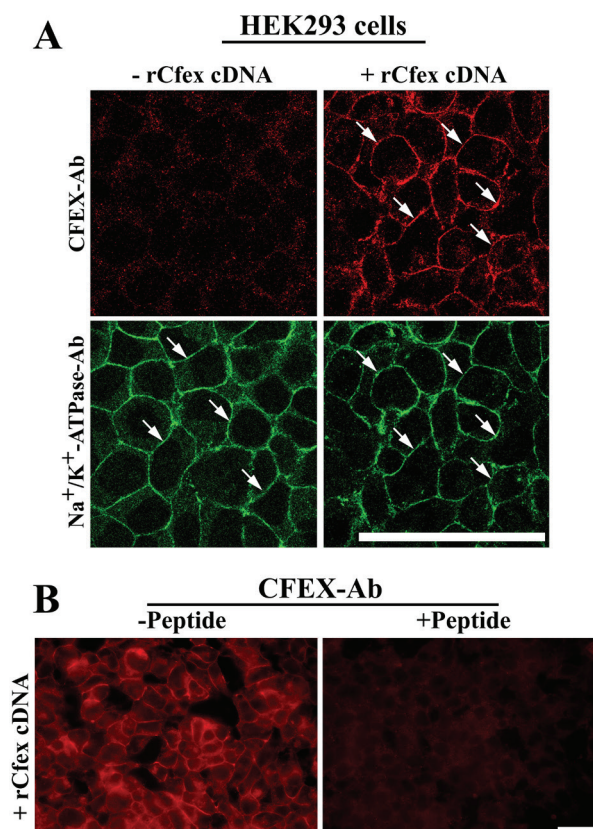
Figure 2 *Testing the specificity of anti-CFEX antibody. A Immunocytochemical testing of CFEX-Ab and Na⁺/K⁺-ATPase-Ab in vector-*
(-rCfex cDNA) and rCfex-*transfected (+rCfex cDNA) HEK293 cells. Arrows denote immunoreactivity in the plasma membrane.*
B *Immunostaining of* rCfex-*transfected cells with CFEX-Ab (-Peptide) and its absence when blocked with the immunising peptide*
(+Peptide). Bar (for all images in the panel), 20 μm. Similar results were obtained in three independent experiments

~120 kDa, which was absent when the same antibody was pre-incubated with its immunising peptide (Figure 5A). In tissue cryosections, the antibody staining was weak in the BBM of the S1/S2 cortex segments of the proximal tubules, stronger in the S3 segments of medullary rays, and the strongest in the S3 segments of the outer stripe (-P) (Figures 5B and C), exhibiting in this way zonal differences (cortex < outer stripe). Other nephron segments remained unstained. No staining was observed with the antibody pre-incubated with its immunising peptide (Figure 5B, +P).

Zonal differences in immunostaining were confirmed in the Western blots of isolated TCM from the kidney cortex and outer stripe; the rCfex-related protein band of ~120 kDa was stronger in the outer stripe (Figure 5D). Its density was 7.3 times higher than in the cortex, whereas the density of the actin band (where the housekeeping protein was used as loading control) was similar in TCM from both zones (Figure 5E).

The expression of rCfex in the rat kidneys also exhibited sex differences (Figure 6). The relative expression of *rCfex* mRNA in the whole kidney, established with qRT-PCR, was ~20 % higher in males than in females (P<0.050) (Figure 6A). This observation was confirmed on the protein level in TCM isolated from the whole male and female kidneys; the rCfex-related protein band (~120 kDa) was

~50 % stronger in males than in females, whereas the actin band had similar density in both sexes (Figure 6B and C). Sex-dependent expression of the rCfex protein was also confirmed by immunostaining the kidney cryosections (Figure 6D); CFEX-Ab-related staining intensity in the cortical and outer stripe tubules was ~30 % and ~4.3 times stronger in males than in females (Figure 6E).

Renal expression of the rCfex protein in prepubertal rats

Western blotting with CFEX-Ab and actin-Ab of the whole kidney TCM from four male and four female prepubertal rats showed ~60 % lower rCfex protein band density than in the adult male and ~100 % higher than in the adult female rats, one of each, that served as comparators. However, we found no sex differences. The density of the actin protein band was also similar between the sexes, but ~55 % lower than in adult animals (Figures 7A and B).

Western blotting was confirmed by the CFEX-Ab-related immunostaining in the kidney cortex and outer stripe in adult and prepubertal male and female rats (Figure 7C). In adult animals it exhibited male-dominant sex differences (stronger staining in the outer stripe), and in prepubertal animals the immunostaining in both tissue zones was weak and similar between the sexes.

Effect of gonadectomy and treatment with sex hormones on the rCfex protein expression in kidneys

In male rats, the rCfex protein band density in Western blots decreased 60 % after castration, whereas actin band density remained unchanged (Figures 8A and B). In tissue cryosections, the CFEX-Ab-related immunostaining was not significantly affected by castration in the cortical tubules, but in the outer stripe tubules staining intensity decreased ~65 % (Figures 8C and D). In female animals, however, the density of protein bands in the whole kidney TCM, and the staining intensity of proximal tubules in tissue cryosections remained unchanged after ovariectomy (data not shown), which clearly suggests that female sex hormones are not responsible for the observed phenomenon.

To confirm male sex hormones as being responsible for sex differences in the renal rCfex expression, castrated males were treated with sunflower oil or oil-solutions of testosterone, oestradiol, or progesterone for two weeks (Figure 9). Western blotting with CFEX-Ab (Figure 9A) and rCfex-related band densitometry (Figure 9B) showed that Cfex protein expression was upregulated by testosterone,

whereas oestradiol and progesterone treatment had no effect. CFEX-Ab-related immunostaining in the cortical tubules showed no changes, but in the outer stripe, testosterone treatment resulted in stronger staining, while oestradiol and progesterone had no effect (Figure 9C).

Urine parameters in sham-operated and gonadectomised male and female rats

In order to estimate if the renal expression of Cfex in sham-operated and gonadectomised male and female rats has any relation to urine excretion of oxalate and a few other parameters known to stimulate (calcium; Ca) or inhibit (citrate) formation of oxalate stones (2), these parameters were determined in urine collected in metabolic cages for 24 h. Table 3 shows that sham-operated females had a significantly lower body mass ($P<0.001$) and higher urine Ca ($P<0.001$) and citrate excretion per day ($P<0.002$) than sham-operated males, when expressed per creatinine.

Castrated males had lower urine volume excretion ($P<0.002$) and higher urine osmolality ($P<0.021$), creatinine ($P<0.012$), and Ca ($P<0.021$) than sham-operated males.
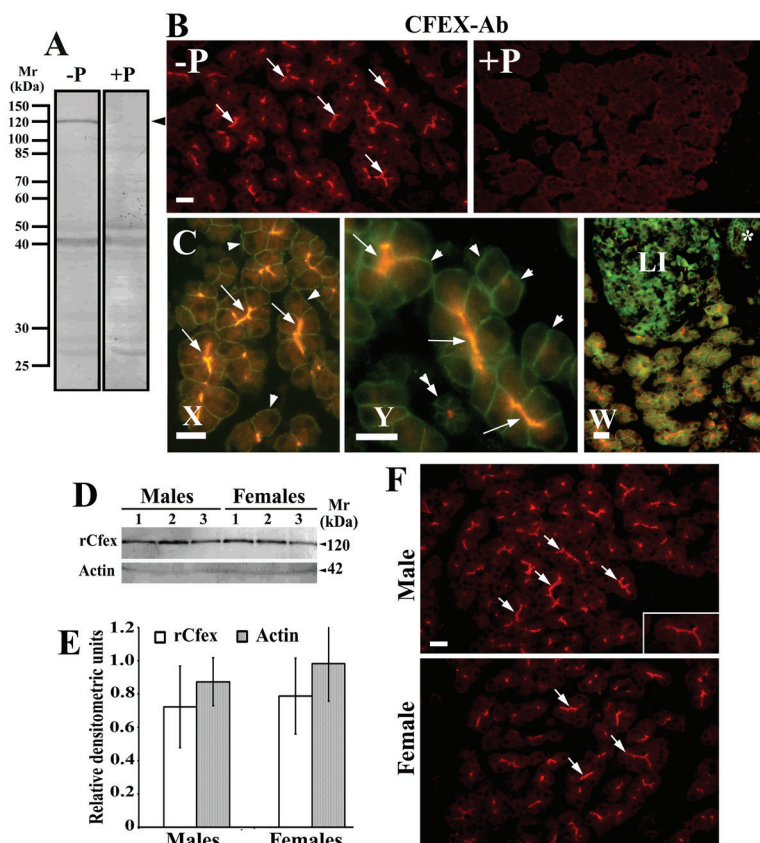
Figure 3 *Immunolocalisation and sex-independent expression of the rCfex protein in the pancreas. A Western blot of total cell membranes (TCM) from the whole male pancreas with CFEX-Ab (-P) and with CFEX-Ab blocked by the immunising peptide (+P). Each lane contained 80 μg of protein. Mr – relative molecular mass. B Tissue cryosection staining with CFEX-Ab (-P), and with CFEX-Ab blocked by its immunising peptide (+P). The arrows point to the staining of the luminal domain in the acini. C (X, Y, W) Double staining with CFEX-Ab (arrows) and Na⁺/K⁺-ATPase-Ab (arrowheads). Double arrowhead points to the initial (intercalated) duct. LI – Langerhans islet; * – larger (intralobular) pancreatic duct. D Western blots of TCM from male and female rat pancreata with CFEX-Ab and actin-Ab. Each lane contained 80 μg of protein from membrane preparations from different rats. E Densitometry (means ±SD; n=3 in each bar) of the protein bands shown in D. Differences in rCfex or actin between males and females were not significant (P>0.05). F CFEX-Ab immunostaining in cryosections of male and female organs. The data represent similar findings in three rats of each sex. Bars (for all images in the respective panel), 20 μm*

Karaica D, et al. Sex-independent expression of Cfex (Slc26a6) in rat pancreas, small intestine, and liver, and male-dominant expression in kidneys
Arh Hig Rada Toksikol 2018;69:286-303

294
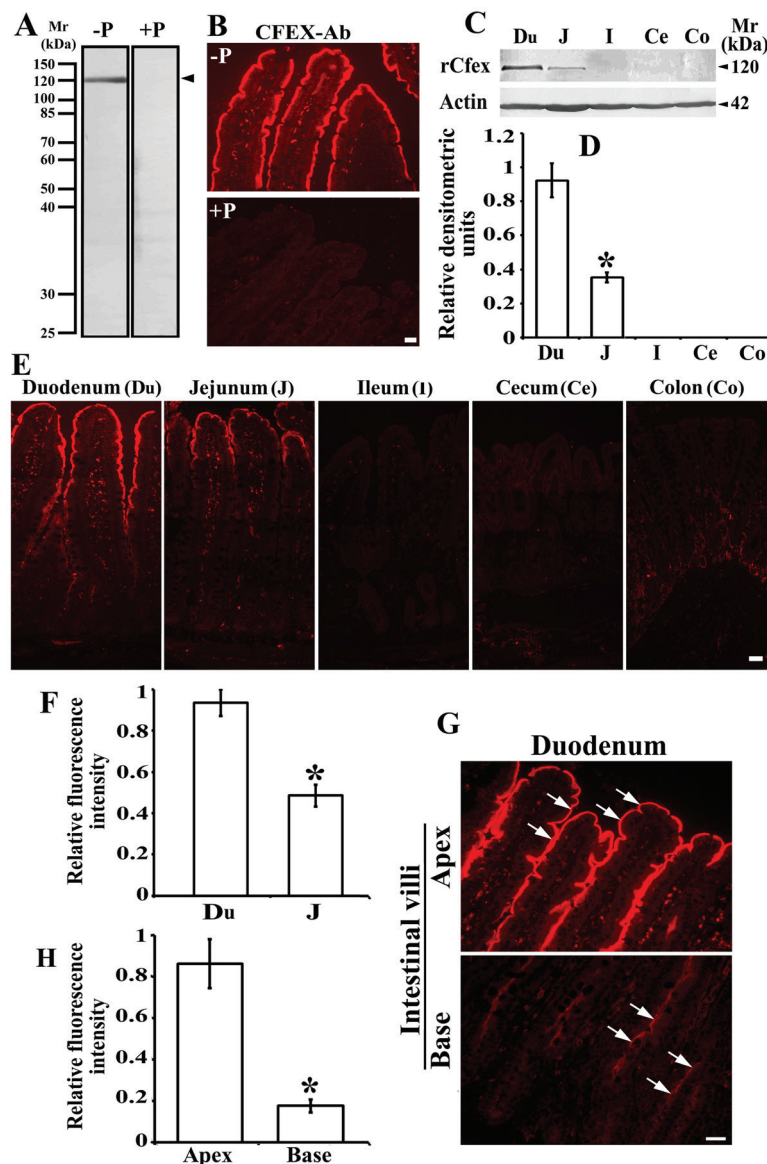
Figure 4 *Expression of the rCfex protein in the intestine. **A** Western blot of total cell membranes (TCM) from duodenal mucosa with CFEX-Ab (-P) and with the same antibody preincubated with its immunising peptide (+P). Each lane contained 80 μg protein. Mr, relative molecular mass. **B** Immunostaining in duodenum with CFEX-Ab (-P) and with the antibody preincubated with its immunising peptide (+P). **C** Representative (out of 3 similar) Western blots of TCM from the intestinal segments with CFEX-Ab and actin-Ab. Du, duodenum; J, jejunum; I, ileum; Ce, cecum; Co, colon. Each lane contained 80 μg protein. **D** Densitometric evaluation of the rCfex-related protein bands shown in B, collected from 3 independent experiments. Shown are means ±SD (n=3 in each bar). *J vs. Du, P<0.001. The density of actin band was similar in all segments (Actin in C; density not measured). **E** Representative (out of 4 similar) immunostaining of the rCfex protein in various intestinal segments. **F** Relative staining intensity in BBM from Du and J. Shown are means ±SD (n=4 in each bar). *J vs. Du, P<0.001. **G** Representative (out of 4 similar) CFEX-Ab-related immunostaining along the duodenal villous apical (apex) and basal (base) parts. **H** Relative staining intensity (means ±SD) in duodenal villi (n=4 in each bar). *Base vs. Apex, P<0.001. Bars (for all images in the respective panel), 20 μm*

Ovariectomised females had higher body mass (P<0.001) and creatinine excretion (P<0.030), but lower urine flow (P<0.019) and citrate excretion (P=0.002), when expressed per creatinine than sham-operated females. However, the concentration of oxalate in urine, as well as the daily excretion of oxalate were similar in sham-operated animals of either sex and were not affected by gonadectomy.

rCfex protein expression in the liver

In the liver of adult rats, the CFEX-Ab-related, immunising peptide-blockable immunoreactivity was localised in the membrane of bile canaliculi (Figure 10A, -P, arrows). This was confirmed by double staining with CFEX-Ab and Na$^+$/K$^+$-ATPase-Ab, where the rCfex protein was stained red in the bile canaliculi (arrows), while the Na$^+$/K$^+$-ATPase α-subunit protein was stained green in the
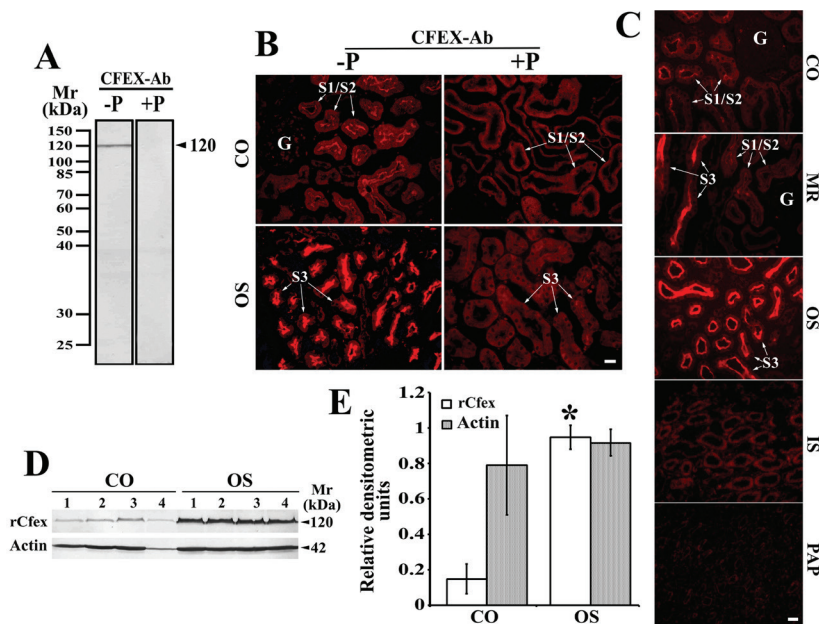
Figure 5 *Immunolocalisation of rCfex in male kidneys; zonal and segmental differences. A Western blot of total cell membranes (TCM) from the whole kidney with CFEX-Ab (-P) and with the same antibody preincubated with its immunising peptide (+P). Each lane contained 80 µg protein. Mr, relative molecular mass. B and C Zonal and segmental differences in immunostaining with CFEX-Ab (-P) and with the same, peptide-blocked antibody (+P). CO, cortex; MR, medullary rays; OS, outer stripe; IS, inner stripe; PAP, papilla (inner medulla); G, glomeruli. S1/S2, proximal tubule convoluted segments. S3, proximal tubule straight segment. Bar (for all images in the respective panel), 20 µm. Data are representative for similar findings in tissue cryosections from 3 male rats. D Western blots of TCM from the kidney cortex and outer stripe with CFEX-Ab and actin-Ab. Actin (~42 kDa protein) was used as a loading control. Each lane contained 80 µg protein from different membrane preparation. E Densitometric evaluation of the protein bands shown in D. Bars show mean ±SD (n=4 in each group). *vs. rCfex in CO, P<0.001*
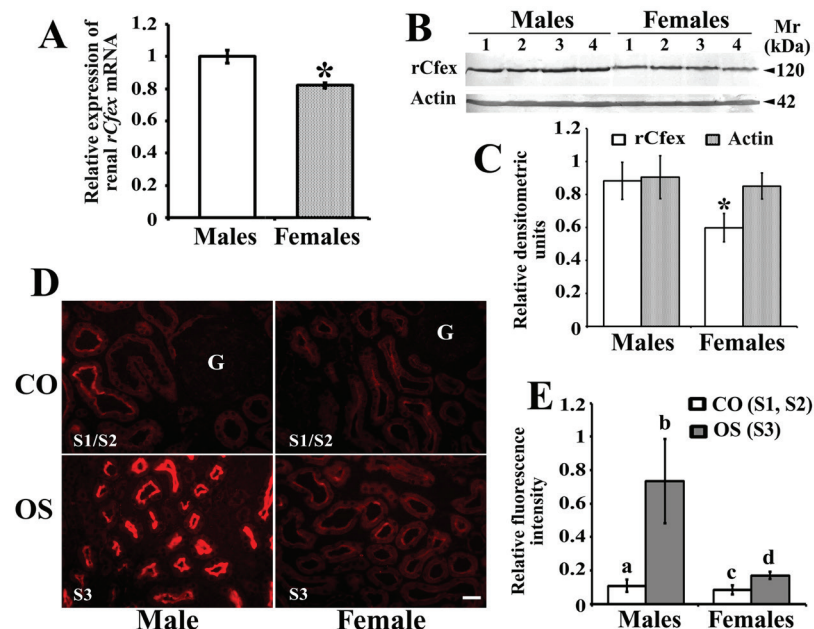
Figure 6 *Sex differences in the expression of* rCfex *mRNA and protein in the kidneys. A qRT-PCR. Relative expression of* rCfex *mRNA from the whole male and female kidneys. Shown are means ±SD (n=4 in each group; *vs. Males, P<0.05). B Western blots of TCM, isolated from the whole male and female kidneys, with CFEX-Ab and actin-Ab. Each lane contained 80 µg protein from different membrane preparation. C Densitometric evaluation of the protein bands shown in B. Bars show mean ±SD (n=4 in each group). *vs. rCfex in Males, P<0.008). D Representative (for four animals of each sex), CFEX-Ab-related immunostaining in proximal tubules in the cortex (CO) and outer stripe (OS) of male and female kidneys. G, glomerulus. S1/S2 and S3, respective proximal tubule segments. Bar (for all images), 20 µm. E Intensity of CFEX-Ab-related staining in the proximal tubule brush-border membrane of cortical (CO) and outer stripe (OS) segments. Shown are means ±SD (n=4 in each group). Statistics: a vs. c, and b vs. d, P<0.003*

Karaica D, et al. Sex-independent expression of Cfex (Slc26a6) in rat pancreas, small intestine, and liver, and male-dominant expression in kidneys
Arh Hig Rada Toksikol 2018;69:286-303

296

hepatocyte sinusoidal membrane (arrowheads). Immunoblotting of TCM isolated from the liver tissue with CFEX-Ab labelled a protein band of ~120 kDa, which was blocked by the immunising peptide (Figure 10B). Furthermore, blots of isolated TCM from male and female livers with CFEX-Ab and actin-Ab (Figure 10C) and densitometry of their protein bands (Figure 10D) showed no sex differences in the abundance. This was supported by similar CFEX-Ab-related staining intensity in tissue cryosections from both sexes (Figure 10E).

DISCUSSION

In this study we established the expression and distribution of *rCfex* mRNA and the rCfex protein in the pancreas, gastrointestinal tract, kidneys, and liver of male and female rats. End-point RT-PCR detected *rCfex* mRNA in the tissue of all tested organs, which confirms earlier findings in humans (12–15), mice (16–18), and rats (10). In our initial immunocytochemical studies in the *rCfex*-transfected cells, the CFEX-Ab was found efficient in immunostaining the rCfex protein in the cell plasma membranes. It also exhibited good efficiency in immunostaining rCfex in tissue cryosections, whereas in the membranes isolated from the investigated rat organs it labelled a single, immunising peptide-blockable protein band of ~120 kDa. This size of the Cfex protein falls within the range detected in various mammalian tissues and cell expression systems (~84 kDa to ~200 kDa) and is attributed to variable posttranslational modifications such as glycosylation (5, 14–16, 18, 23, 29–32). In various

experimental conditions, the density of ~120 kDa protein band and CFEX-ab-related staining distribution and intensity in the respective organs matched, indicating their protein-related origin. Sex differences (males > females) in the expression of both *rCfex* mRNA and the protein were detected only in the kidneys.

Our finding of the rCfex (PAT-1) protein in the rat pancreas confirms previous reports for human and animal pancreas (4, 8, 9, 13, 20, 21). Studies on microperfused pancreatic ducts and ductal cell lines, suggest that Cfex (regulated by CFTR) is the major apical Cl^-/HCO_3^- exchanger in mammalian pancreatic ducts and that it contributes to the secretion of HCO_3^--rich fluid (4, 6, 21, 49). However, in contrast to previous immunocytochemical and functional findings of Cfex in the luminal membrane of interlobular duct cells of human (13), guinea pig (9), and mouse (6) pancreas, our study demonstrated: a) no CFEX-Ab-related immunoreactivity in the cells of intralobular and larger ducts, b) weak immunoreactivity in the cell luminal domain of initial (intercalated) ducts, and c) strong immunoreactivity in the luminal domain of acinar cells. In many cells we also observed numerous weakly rCfex-positive intracellular organelles, which suggests that the level of the rCfex protein in the apical cell membrane may be controlled by vesicle recycling and possibly regulated by endo- and exocytosis.

As detected by qRT-PCR, *rCfex* mRNA in various intestinal segments revealed the highest expression was in the duodenum, lower in the jejunum, and even lower in the ileum, whereas in other segments (stomach, cecum, and proximal colon) the expression was negligible. These results

Table 3 *Body mass, urine excretion, and urine biochemical parameters in the sham-operated and gonadectomised male and female rats*

Parameter	Males		Females	
	Sham-operated	Castrated	Sham-operated	Ovariectomised
Body mass (g)	289±25	266±29	193±13‡	232±14§
Urine parameters Volume (mL/24 h)	37.6±10.4	25.1±8.9	35.6±12.8	26.2±12.2
Flow (mL/24 h kg bm)	130±33	94±31†	185±68†	113±52‖
Osmolality (mosm kg^{-1})	267±78	440±188†	266±104	497±373
pH	7.0±0.20	7.3±0.63	6.8±0.59	6.7±0.26
Creatinine, mmol L^{-1}	3.4±4.17	3.5±1.68	2.4±2.44	3.9±3.19
µmol/24 h kg bm	244±34	293±42†	259±41	306±47‖
Calcium, mmol L^{-1}	0.46±0.20	0.76±0.29†	1.31 ±0.82†	1.24±0.86
mmol/24 h kg bm	3.8±1.76	9.4±5.90†	8.5±7.14	23.7±34.09
Citrate, mmol L^{-1}	1.15±0.34	2.15±1.36†	1.45±0.53	2.11±1.23
µmol/24 h kg bm	142±34	176±46	241±47‡	186±81
mmol/mol creatinine	593±168	597±118	949±239†	593±202‖
Oxalate, µmol L^{-1}	182±90	256±135	203±167	219±105
µmol/24 h kg bm	20.3±5.1	20.7±4.1	19.0±7.1	20.1±5.6
mmol/mol creatinine	83±14.1	71±11.7	73±29.6	65±14.8

The results are presented as means ±SD of body mass and biochemical parameters in 24-h urine collected from 9 to 10 animals in each experimental group. †P=0.001-0.047 vs. sham-operated males; ‡P<0.001 vs. sham-operated males; §P<0.001 vs. sham-operated females; ‖P=0.001-0.030 vs. sham-operated females. Other comparisons were not statistically significant (P>0.05)
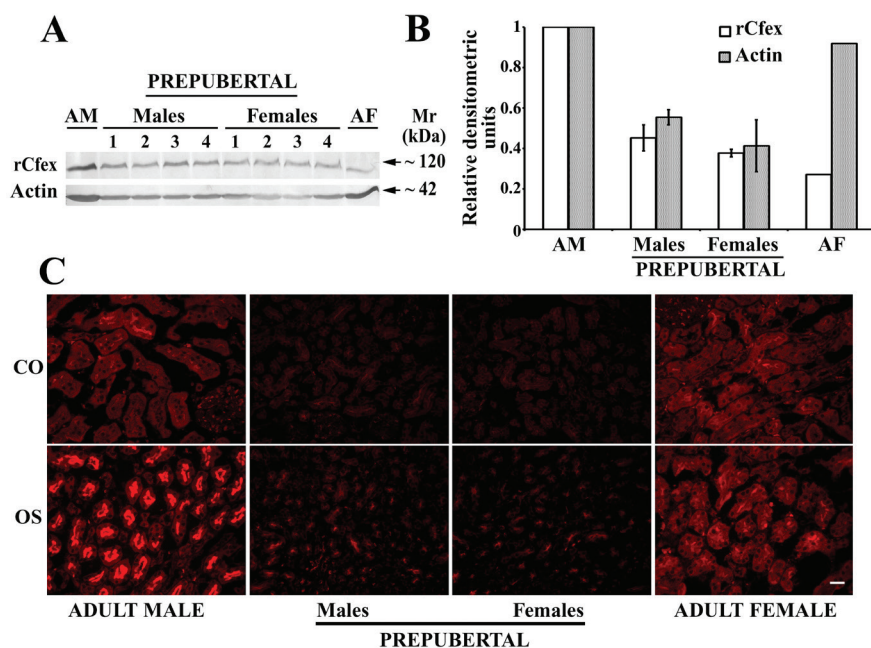
Figure 7 *Immunolocalisation of the rCfex protein in the kidneys of prepubertal male and female rats; comparison with adult animals. A Western blots of total cell membranes (80 µg protein/lane), isolated from the whole kidneys from 4 male and 4 female prepubertal rats, and from one adult male (AM) and female (AF) rat, blotted with CFEX-Ab and actin-Ab. B Densitometric evaluation of the protein bands shown in A. Data for adult rats are from a single animal, whereas the data for prepubertal animals are means ±SD (n=4 in each group). Statistics for the rCfex and actin data in prepubertal rats: Males* vs. *Females, N.S. (P>0.05). C Representative (out of 3 similar) rCfex-Ab-related immunostaining in the kidney cortex (CO) and outer stripe (OS) in adult and prepubertal male and female rats. Bar (for all images), 20 µm*

differ from the Northern hybridisation data in mouse intestine, showing this sequence of expression: duodenum=jejunum > ileum > proximal colon > cecum > distal colon (17, 18). Our immunochemical data of the intestinal rCfex matched the mRNA expression, showing the rCfex protein in the BBM of duodenal and jejunal enterocytes (duodenum > jejunum). In other segments, including the stomach, the rCfex protein could not been visualised. In the mouse stomach, the mCfex protein was previously detected with a different antibody and found colocalised with gastric H^+-K^+-ATPase in parietal cells (22). This suggests that intestinal *Cfex* mRNA and protein expression implies species differences between rats and mice.

The role of Cfex in the murine small intestine has been functionally defined in studies on wild type and *mCfex* knockout mice, in *Cfex*-transfected cell lines and in *Xenopus* oocytes (5, 7, 18, 26, 28, 29, 31). Two of them also described species differences in kinetic properties between the mouse and human Cfex/CFEX proteins. The mCfex-mediated Cl^-/oxalate^{2-} exchange was electrogenic with high affinity for Cl^-, whereas the human exchanger was electroneutral (2Cl^-/oxalate^{2-}), with low affinity for Cl^- (5, 50). Previously published data indicates that duodenal and ileal Cfex could mediate absorption of luminal Cl^- or SO_4^{2-} in exchange for secreted HCO_3^- or oxalate (7, 26, 28, 29). With the latter function, the exchanger should significantly contribute in eliminating oxalate from the body (26, 34), thus preventing

the development of hyperoxalemia, which can lead to subsequent hyperoxaluria and Ca-oxalate nephrolithiasis, as has been demonstrated in the *mCfex* knockout mouse model (32, 34, 51).

The segment-related expression of Cfex protein along the renal proximal tubule (S1/S2 in the cortex << S3 in medullary rays and outer stripe) and sex differences in the expression of *Cfex* mRNA and protein (males > females) found in our study in rats have not been previously reported for other species. In a study using northern hybridisation (10), *rCfex/PAT-1* mRNA was highly expressed in the kidney cortex and weakly in the outer and inner medulla, whereas immunocytochemical staining localised the rCfex protein in the proximal tubule BBM. The mCfex protein was also stained in the BBM of the proximal tubules (11, 16), but in humans, CFEX was detected in the distal segments of the proximal tubules and in several more distal nephron parts (12), which all points to species differences in the nephron localisation of this transporter between rodents and humans. In various transport studies, performed in microperfused proximal tubules from wild type and *mCfex* knockout mice (10, 11, 25, 29), isolated BBM (10, 11, 25, 52), and *mCfex*- and *CFEX*-transfected *Xenopus* oocytes (5, 50), the renal Cfex/CFEX was shown to function predominantly as Cl^-/HCO_3^- or Cl^-/oxalate exchanger, thus serving in reabsorption of Cl^- and secretion of HCO_3^- and oxalate. As shown in the mouse kidney, a strongly diminished transport of oxalate in renal BBM vesicles

Karaica D, et al. Sex-independent expression of Cfex (Slc26a6) in rat pancreas, small intestine, and liver, and male-dominant expression in kidneys
Arh Hig Rada Toksikol 2018;69:286-303

298

isolated from *mCfex*-knockout animals, and much higher affinity of renal mCfex for oxalate than for HCO_3^- (25, 52) indicate Cl^-/oxalate exchange as the primary role of the renal transporter.

Two phenomena related to our findings of male-dominant testosterone-induced rCfex protein expression in the kidney deserve particular attention. One is the segment-dependent abundance of rCfex, which is in S3 much higher than in S1/S2. Previous studies assumed that oxalate elimination via proximal tubule cells was mediated by the concerted action of the basolateral Sat-1, which pumps SO_4^{2-} out and oxalate into the cell, and luminal Cfex, which transports oxalate into the tubule lumen in exchange for Cl^- [reviewed in (1, 2, 35)]. In the rat kidney, this pattern may be valid for S1/S2 segments, which exhibit male-dominant expression of both rSat-1 (37, 40) and rCfex (this study), but is not entirely true for the S3 segments, where apical rCfex expression is higher (this study) and basolateral rSat-1 lower (37, 53). It remains for the future studies to resolve the physiological role of the male-dominant rCfex expression in the S3 segment in secretion or reabsorption of oxalate and other related anions.

The other phenomenon are strong male-dominant sex differences in rCfex expression along the entire proximal tubule, which may be relevant to the well-known male-dominant prevalence of urolithiasis in humans and animals [reviewed in (1, 2, 35)]. According to the urine parameters in Table 3, similar urine concentrations and 24-h excretion of oxalate in the sham-operated and gonadectomised male and female rats suggests no apparent relation between oxalate excretion and renal rCfex expression, which is in contradiction with some previously reported studies (26, 29, 34).

Male-dominant expression of renal rCfex in our study may play a role in hyperoxalaemic conditions such as chronic renal failure (54, 55), inflammatory bowel disease, small bowel resection (28), and urolithiasis induced by ethylene glycol (EG) in rats (40). Several studies have shown that male rats have a predilection toward kidney stones and that testosterone enhances while oestrogen inhibits urinary stone formation in normal and EG-treated animals (56–58), but the expression and the role of Cfex was not investigated in those studies. However, higher excretion of citrate in healthy females than males [(40) and this study] may point to a major protective mechanism against the formation of Ca-oxalate crystals. An *in vitro* study by Ohana et al. (32) showed that mCfex can interact with and inhibit the activity of sodium-dicarboxylate cotransporter mNaDC-1/Slc13a2 located in the proximal tubule BBM, which reabsorbs filtrated citrate. *In vivo*, such inhibition could result in citrate retention in the tubular fluid, which would bind Ca^{2+} and ensure safe oxalate elimination through urine (32). The 24-h urine in our previous (40) and present study consistently showed significant sex differences (males<females) in the excreted citrate but not oxalate. These differences disappeared with

ovariectomy (this study), suggesting that in rats, female sex hormones regulate (stimulate) citrate excretion by modulating the activity and/or expression of NaDC-1, while the Cfex remains unaffected. EG-induced urolithiasis, hyperoxaluria, and hypocitraturia in rats (40) generated conditions for the formation of Ca-oxalate crystals in male but not female animals. Since male rats exhibit higher renal expression of the rCfex protein than females (this study), it is possible that this and several other conditions with hyperoxaluria and Ca-oxalate urolithiasis may involve an interaction between Cfex and NaDC-1, such as inflammatory bowel disease and conditions resulting from small bowel resection (28, 35).

Earlier Northern blotting and/or RT-PCR studies have detected *CFEX/Cfex* mRNA in the liver of humans (13–15) and mice (16), but no CFEX/Cfex protein has been localised to hepatocytes in these species so far. Following up on our preliminary report in the rat liver of a few years ago (2), we have now confirmed its exclusive presence in the bile canaliculi, where it may play a role in elimination of oxalate from hepatocytes into bile. Judging by the CFEX-Ab-related immunostaining intensity its expression was sex-independent. Liver is the organ with the largest capacity of producing oxalate from various precursors [reviewed in (2, 35)]. This is particularly clear in hepatectomised rats, whose production of oxalate from the precursor glycolate dropped more than 80 % (59). Being an end-product of metabolism and toxic for the cell, most of oxalate is removed from the hepatocytes via Sat-1-mediated SO_4^{2-}/oxalate exchange located in the sinusoidal membrane [reviewed in (1, 2, 35)]. In an experimental rat model of EG-induced hyperoxaluria, the expression of *rSat-1* mRNA and rSat-1 protein in the liver (and kidneys) exhibited only limited changes (39, 40), whereas in *Sat-1* knockout mice with hyperoxalaemia, hyperoxaluria, and nephrolithiasis (33) the mode of oxalate elimination from hepatocytes has not been explained. Previous transport studies by Meier et al. (60) in canalicular plasma membrane vesicles isolated from the rat liver showed the presence of HCO_3^-/SO_4^{2-}, HCO_3^-/oxalate and SO_4^{2-}/oxalate exchange. According to Boyer (61), HCO_3^- is secreted into the bile in exchange for Cl^- by anion exchanger 2 (AE2/SLC4A2) located in the bile canalicular membrane, and the out-to-in gradient of bicarbonate may drive SO_4^{2-} and oxalate exit by another exchanger in the same membrane, possibly Cfex. We therefore propose that oxalate produced in the liver can leave the hepatocyte via sinusoidal Sat-1 (2, 37) and canalicular Cfex. The Cfex-mediated excretion of oxalate may be low under physiological conditions and may increase in case of impaired oxalate clearance, as shown in rats with kidney failure (54). For example, in nephrectomised rats, biliary secretion of oxalate was reported to account for ~18 % of the total clearance (62). Future experiments will need to identify changes in hepatic Cfex expression and its role in hyperoxalaemia and hyperoxaluria.
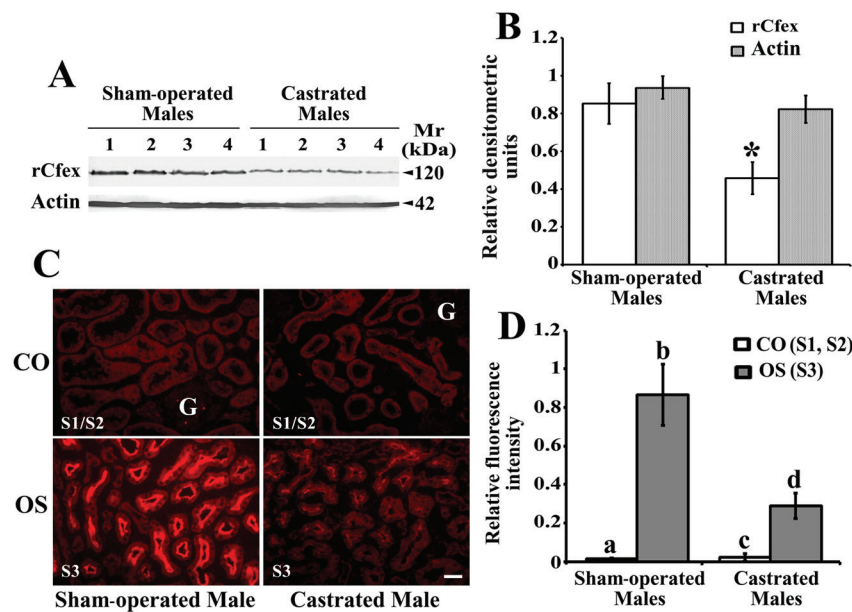
Figure 8 *Effect of gonadectomy on the rCfex protein expression in male kidneys. A Western blots of the whole kidney total cell membranes, isolated from 4 sham-operated and 4 castrated animals, with CFEX-Ab and actin-Ab. Each lane contained 80 µg protein. B Densitometric evaluation of the protein bands shown in A. Shown are means ±SD (n=4 in each bar). *vs. rCfex in sham-operated males, P<0.002. The actin band had similar density in the membranes from both groups (P>0.05). C rCfex-Ab-related immunostaining in the cortical (CO) and outer stripe (OS) proximal tubule segments (S1/S2 and S3) from sham-operated and castrated animals. G, glomeruli. Bar (for all images), 20 µm. Data are representative for 3 animals in each group. D Staining intensity in the brush-border membrane of cortical (CO, S1/S2) and outer stripe (OS, S3) proximal tubule segments. Shown are relative fluorescence intensities (means ±SD; n=3 in each bar). Statistics: In CO, a vs. c, N.S. (P>0.05); In OS, b vs. d, P<0.005*
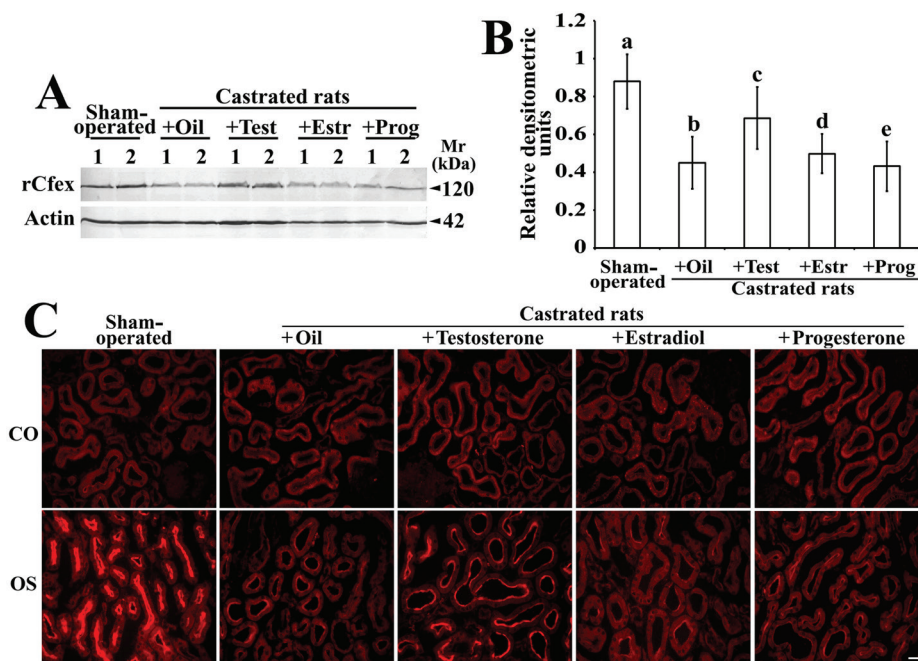
Figure 9 *Effect of sex hormone treatment in castrated rats on renal rCfex protein expression. A Western blots (representative for 2 different sets of membrane preparations) of total cell membranes, isolated from the outer stripe of sham-operated and castrated rats treated with sunflower oil or sex hormones (Test, testosterone; Estr, oestrogen; Prog, progesterone) for two weeks, with CFEX-Ab and actin-Ab. Each lane contained 80 µg protein. B Densitometric evaluation of the bands shown in A. Shown are means ±SD of the data collected from two independent experiments (n=4 in each group); Statistics: a vs. b, d or e; b vs. c, and c vs. d or e, P<0.001; Other relationships, N.S. (P>0.05). The actin protein band was not changed by the treatments (A). C The CFEX-Ab-related immunostaining in cortical (CO) and outer stripe (OS) proximal tubule segments. Images are representative for similar findings in 3 animals in each group. Bar (for all images), 20 µm*

Karaica D, et al. Sex-independent expression of Cfex (Slc26a6) in rat pancreas, small intestine, and liver, and male-dominant expression in kidneys
Arh Hig Rada Toksikol 2018;69:286-303

300
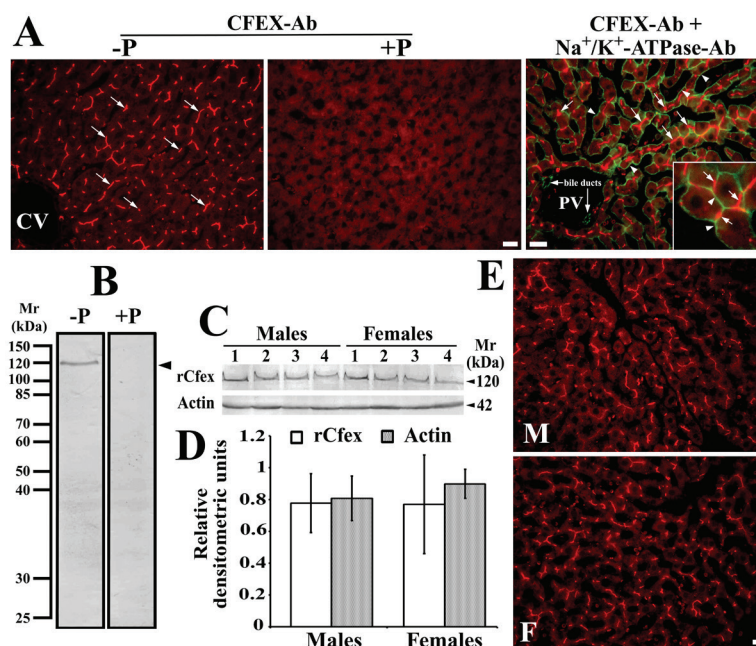
Figure 10 *Immunolocalisation and sex-independent expression of the rCfex protein in the liver. **A** CFEX-Ab-related immunoreactivity in hepatocytes. The immunostaining with CFEX-Ab (-P) and with the immunising peptide-blocked antibody (+P). The colour figure (and insert) shows a representative, double-stained cryosection with CFEX-Ab (red fluorescence) and Na+/K+-ATPase-Ab (green fluorescence). Arrows, rCfex in bile canaliculi; arrowheads, Na+/K+-ATPase in sinusoidal membrane; CV, central vein; PV, portal vein. **B** Western blot of total cell membranes (TCM) from the liver tissue with CFEX-Ab (-P) and with the same, immunising peptide-blocked antibody (+P). **C** Western blots of TCM with CFEX-Ab and actin-Ab. Each lane contained 80 µg protein of different membrane preparations. **D** Densitometric evaluation of the bands shown in B. Shown are means ±SD (n=4 in each group). Statistics: Males vs. Females (rCfex or actin), N.S. (P>0.05). **E** The CFEX-Ab-related immunostaining in male and female livers, representing similar findings in tissue cryosections from 3 rats of each sex. Bars (for all images in the respective panel), 20 µm*

In conclusion, by applying the commercial polyclonal anti-CFEX antibody (sc-26728) in rat tissues, the putative rCfex protein was detected in a few known localizations (duodenal and jejunal BBM, luminal domain of pancreatic intercalated ducts, BBM in proximal tubules), and a few previously unknown localizations (bile canalicular membrane in hepatocytes, and apical membrane and intracellular organelles in pancreatic acinar cells). The expression of rCfex was found sex-dependent only in kidneys, exhibiting a strong male-dominant expression driven by androgen stimulation after the puberty. The described localizations may be important in handling oxalate and related anions in physiological and pathophysiological conditions. However, while the applied antibody worked well by immunocytochemistry in tissue cryosection, by immunoblotting it labelled no protein in the membranes isolated from transfected cells, but labelled the protein band of ~120 kDa in the membranes isolated from various organs. In our preliminary studies, we have also tested the two other commercially-available anti-Cfex antibodies, one polyclonal (sc-26735) and one monoclonal (sc-515230), which are supposed to label Cfex in rodents; both were ineffective in our immunochemical experiments, and thus, we could not prove with an independent approach if the ~120 kDa protein was strictly related to rCfex. Yet, the CFEX-Ab-related density pattern of ~120 kDa protein fully matched the pattern of immunostaining in various

tissues, indicating the possibility that both, the protein band and immunostaining reflect the same protein expression.

Author contributions

DK and DB contributed equally to this work. DB, TS, GB, BCB and IS designed the concept of study. DK, DB, JL, ML, VM, IVM, HB, CMH-K, JID, MLJ, TS, and ŽV performed experiments. DK, DB, and IS analysed and interpreted the data and prepared and approved the final version of the manuscript. All authors read and approved the manuscript.

Conflict of interest

None to declare.

Abbreviations

bm – body mass; BBM – brush border membrane; BCP – 5-bromo-4-chloro-3-indolyl-phosphate; cDNA – complementary deoxyribonucleic acid; CFEX (Cfex)/

SLC26A6 (Slc26a6) – chloride-formate exchanger/member A6 of the solute carrier family 26; CFEX-Ab – chloride-formate exchanger antibody; DAG-CY3 – cyanine 3-labelled donkey anti-goat IgG; EG – ethylene glycol; GAM-AP – goat anti-mouse IgG; GAM-FITC – fluorescein isothiocyanate-labelled goat anti-mouse IgG; HEK293 – human embrionic kidney cell line 293; NaDC-1/Slc13a2 – sodium dicarboxylate cotransporter 1/member a2 of the solute carrier family 13; Mr – relative molecular mass; Na$^+$/K$^+$-ATPase – sodium-potassium adenosine triphosphatase; NBT – nitro blue tetrazolium; PAT-1 – putative anion transporter 1; PBS – phosphate buffer solution; PEI – polyethyleneimine; PFA – p-formaldehyde; RAG-AP – alkaline phosphatase-labelled rabbit anti-goat IgG; *Hprt1* – hypoxanthine phosphoribosyltransferase 1 housekeeping gene; ROI – regions of interest; *β-actin* – beta actin housekeeping gene; S1-3 – segments 1, 2, and 3 of the kidney proximal tubule; Sat-1/Slc26a1 – sulphate anion transporter; SDS-PAGE – sodium dodecyl sulphate polyacrylamide gel electrophoresis; TCM – total cell membranes

REFERENCES

1. Alper SL, Sharma AK. The SLC26 gene family of anion transporters and channels. Mol Aspects Med 2013;34:494-515. doi: 10.1016/j.mam.2012.07.009

2. Brzica H, Breljak D, Burckhardt BC, Burckhardt G, Sabolić I. Oxalate: from the environment to kidney stones. Arh Hig Rada Toksikol 2013;64:609-30. doi: 10.2478/10004-1254-64-2013-2428

3. Mount DB, Romero MF. The SLC26 gene family of multifunctional anion exchangers. Pflug Arch Eur J Phy 2004;447:710-21. doi: 10.1007/s00424-003-1090-3

4. Steward MC, Ishiguro H. Molecular and cellular regulation of pancreatic duct cell function. Curr Opin Gastroen 2009;25:447-53. doi: 10.1097/MOG.0b013e32832e06ce

5. Chernova MN, Jiang L, Friedman DJ, Darman RB, Lohi H, Kere J, Vandorpe DH, Alper SL. Functional comparison of mouse slc26a6 anion exchanger with human SLC26A6 polypeptide variants: differences in anion selectivity, regulation, and electrogenicity. J Biol Chem 2005;280:8564-80. doi: 10.1074/jbc.M411703200

6. Ishiguro H, Namkung W, Yamamoto A, Wang Z, Worrell RT, Xu J, Lee MG, Soleimani M. Effect of Slc26a6 deletion on apical Cl$^-$/HCO$_3^-$ exchanger activity and cAMP-stimulated bicarbonate secretion in pancreatic duct. Am J Physiol-Gastr L 2007;292:G447-55. doi: 10.1152/ajpgi.00286.2006

7. Simpson JE, Schweinfest CW, Shull GE, Gawenis LR, Walker NM, Boyle KT, Soleimani M, Clarke LL. PAT-1 (Slc26a6) is the predominant apical membrane Cl$^-$/HCO$_3^-$ exchanger in the upper villous epithelium of the murine duodenum. Am J Physiol-Gastr L 2007;292:G1079-88. doi: 10.1152/ajpgi.00354.2006

8. Stewart AK, Shmukler BE, Vandorpe DH, Reimold F, Heneghan JF, Nakakuki M, Akhavein A, Ko S, Ishiguro H, Alper SL. SLC26 anion exchangers of guinea pig pancreatic duct: molecular cloning and functional characterization. Am J Physiol-Cell Ph 2011;301:C289-303. doi: 10.1152/ajpcell.00089.2011

9. Stewart AK, Yamamoto A, Nakakuki M, Kondo T, Alper SL, Ishiguro H. Functional coupling of apical Cl$^-$/HCO$_3^-$ exchange with CFTR in stimulated HCO3$^-$ secretion by guinea pig interlobular pancreatic duct. Am J Physiol-Gastr L 2009;296:G1307-17. doi: 10.1152/ajpgi.90697.2008

10. Petrović S, Ma L, Wang Z, Soleimani M. Identification of an apical Cl$^-$/HCO3$^-$ exchanger in rat kidney proximal tubule. Am J Physiol-Cell Ph 2003;285:C608-17. doi: 0.1152/ajpcell.00084.2003

11. Thomson RB, Wang T, Thomson BR, Tarrats L, Girardi A, Mentone S, Soleimani M, Kocher O, Aronson PS. Role of PDZK1 in membrane expression of renal brush border ion exchangers. P Natl Acad Sci USA 2005;102:13331-6. doi: 10.1073/pnas.0506578102

12. Kujala M, Tienari J, Lohi H, Elomaa O, Sariola H, Lehtonen E, Kere J. SLC26A6 and SLC26A7 anion exchangers have a distinct distribution in human kidney. Nephron Exp Nephrol 2005;101:e50-8. doi: 10.1159/000086345

13. Lohi H, Kujala M, Kerkelä E, Saarialho-Kere U, Kestilä M, Kere J. Mapping of five new putative anion transporter genes in human and characterization of SLC26A6, a candidate gene for pancreatic anion exchanger. Genomics 2000;70:102-12. doi: 10.1006/geno.2000.6355

14. Lohi H, Lamprecht G, Markovich D, Heil A, Kujala M, Seidler U, Kere J. Isoforms of SLC26A6 mediate anion transport and have functional PDZ interaction domains. Am J Physiol-Cell Ph 2003;284:C769-79. doi: 10.1152/ajpcell.00270.2002

15. Waldegger S, Moschen I, Ramirez A, Smith RJ, Ayadi H, Lang F, Kubisch C. Cloning and characterization of SLC26A6, a novel member of the solute carrier 26 gene family. Genomics 2001;72:43-50. doi: 10.1006/geno.2000.6445

16. Knauf F, Yang CL, Thomson RB, Mentone SA, Giebisch G, Aronson PS. Identification of a chloride-formate exchanger expressed on the brush border membrane of renal proximal tubule cells. P Natl Acad Sci USA 2001;98:9425-30. doi: 10.1073/pnas.141241098

17. Xie Q, Welch R, Mercado A, Romero MF, Mount DB, Michael F. Molecular characterization of the murine Slc26a6 anion exchanger: functional comparison with Slc26a1. Am J Physiol-Renal 2002;283:F826-38. doi: 10.1152/ajprenal.00079.2002

18. Wang Z, Petrović S, Mann E, Soleimani M. Identification of an apical Cl$^-$/HCO$_3^-$ exchanger in the small intestine. Am J Physiol-Gastr L 2002;282:G573-9. doi: 10.1152/ajpgi.00338.2001

19. Gholami K, Muniandy S, Salleh N. Progesterone downregulates oestrogen-induced expression of CFTR and SLC26A6 proteins and mRNA in rats' uteri. J Biomed Biotechnol 2012;2012:596084. doi: 10.1155/2012/596084

20. García M, Hernández-Lorenzo P, San Román JI, Calvo JJ. Pancreatic duct secretion: experimental methods, ion transport mechanisms and regulation. J Physiol Biochem 2008;64:243-57. doi: 10.1007/BF03178846

21. Saint-Criq V, Gray MA. Role of CFTR in epithelial physiology. Cell Mol Life Sci 2016;74:93-115. doi: 10.1007/s00018-016-2391-y

22. Petrović S, Wang Z, Ma L, Seidler U, Forte JG, Shull GE, Soleimani M. Colocalization of the apical Cl$^-$/HCO$_3^-$

Karaica D, et al. Sex-independent expression of Cfex (Slc26a6) in rat pancreas, small intestine, and liver, and male-dominant expression in kidneys
Arh Hig Rada Toksikol 2018;69:286-303

302

exchanger PAT1 and gastric H-K-ATPase in stomach parietal cells. Am J Physiol-Gastr L 2002;283:G1207-16. doi: 0.1152/ajpgi.00137.2002

23. Alvarez BV, Kieller DM, Quon AL, Markovich D, Casey JR. Slc26a6: a cardiac chloride-hydroxyl exchanger and predominant chloride-bicarbonate exchanger of the mouse heart. J Physiol 2004;561:721-34. doi: 10.1113/jphysiol.2004.077339

24. Kim HJ, Myers R, Sihn C-R, Rafizadeh S, Zhang X-D. Slc26a6 functions as an electrogenic Cl⁻/HCO3⁻ exchanger in cardiac myocytes. Cardiovasc Res 2013;100:383-91. doi: 10.1093/cvr/cvt195

25. Aronson PS. Essential roles of CFEX-mediated Cl⁻-oxalate exchange in proximal tubule NaCl transport and prevention of urolithiasis. Kidney Int 2006;70:1207-13. doi: 10.1038/sj.ki.5001741

26. Freel RW, Hatch M, Green M, Soleimani M. Ileal oxalate absorption and urinary oxalate excretion are enhanced in Slc26a6 null mice. Am J Physiol-Gastr L 2006;290:G719-28. doi: 10.1152/ajpgi.00481.2005

27. Greeley T, Shumaker H, Wang Z, Schweinfest CW, Soleimani M. Downregulated in adenoma and putative anion transporter are regulated by CFTR in cultured pancreatic duct cells. Am J Physiol-Gastr L 2001;281:G1301-8. doi: 10.1152/ajpgi.2001.281.5.G1301

28. Knauf F, Ko N, Jiang Z, Robertson WG, Van Itallie CM, Anderson JM, Aronson PS. Net intestinal transport of oxalate reflects passive absorption and SLC26A6-mediated secretion. J Am Soc Nephrol 2011;22:2247-55. doi: 10.1681/ASN.2011040433

29. Wang Z, Wang T, Petrović S, Tuo B, Riederer B, Barone SL, Lorenz JN, Seidler U, Aronson PS, Soleimani M. Renal and intestinal transport defects in Slc26a6-null mice. Am J Physiol-Cell Ph 2005;288:C957-65. doi: 10.1152/ajpcell.00505.2004

30. Thomson RB, Thomson CL, Aronson PS. N-glycosylation critically regulates function of oxalate transporter SLC26A6. Am J Physiol-Cell Ph 2016;311:C866-73. doi: 10.1152/ajpcell.00171.2016

31. Hassan HA, Mentone S, Karniski LP, Rajendran VM, Aronson PS. Regulation of anion exchanger Slc26a6 by protein kinase C. Am J Physiol-Cell Ph 2007;292:C1485-92. doi: 10.1152/ajpcell.00447.2006

32. Ohana E, Shcheynikov N, Moe OW, Muallem S. SLC26A6 and NaDC-1 transporters interact to regulate oxalate and citrate homeostasis. J Am Soc Nephrol 2013;24:1617-26. doi: 10.1681/ASN.2013010080

33. Dawson PA, Russell CS, Lee S, McLeay SC, van Dongen JM, Cowley DM, Clarke LA, Markovich D. Urolithiasis and hepatotoxicity are linked to the anion transporter Sat1 in mice. J Clin Invest 2010;120:706-12. doi: 10.1172/JCI31474

34. Jiang Z, Asplin JR, Evan AP, Rajendran VM, Velazquez H, Nottoli TP, Binder HJ, Aronson PS. Calcium oxalate urolithiasis in mice lacking anion transporter Slc26a6. Nat Genet 2006;38:474-8. doi: 10.1038/ng1762

35. Robijn S, Hoppe B, Vervaet BA, D'Haese PC, Verhulst A. Hyperoxaluria: a gut-kidney axis? Kidney Int 2011;80:1146-58. doi: 10.1038/ki.2011.287

36. Romero V, Akpinar H, Assimos DG. Kidney stones: a global picture of prevalence, incidence, and associated risk factors. Rev Urol 2010;12:e86-96. doi: 10.3909/riu0459

37. Brzica H, Breljak D, Krick W, Lovrić M, Burckhardt G, Burckhardt BC, Sabolić I. The liver and kidney expression of sulfate anion transporter sat-1 in rats exhibits male-dominant gender differences. Pflug Arch Eur J Phy 2009;457:1381-92. doi: 10.1007/s00424-008-0611-5

38. Ko N, Knauf F, Jiang Z, Markovich D, Aronson PS. Sat1 is dispensable for active oxalate secretion in mouse duodenum. Am J Physiol-Cell Ph 2012;303:C52-7. doi: 10.1152/ajpcell.00385.2011

39. Freel RW, Hatch M. Hyperoxaluric rats do not exhibit alterations in renal expression patterns of Slc26a1 (SAT1) mRNA or protein. Urol Res 2012;40:647-54. doi: 10.1007/s00240-012-0480-4

40. Breljak D, Brzica H, Vrhovac I, Micek V, Karaica D, Ljubojević M, Sekovanić A, Jurasović J, Rašić D, Peraica M, Lovrić M, Schnedler N, Henjakovic M, Wegner W, Burckhardt G, Burckhardt BC, Sabolić. In female rats, ethylene glycol treatment elevates protein expression of hepatic and renal oxalate transporter sat-1 (Slc26a1) without inducing hyperoxaluria. Croat Med J 2015;56:447-59. doi: 10.3325/cmj.2015.56.447

41. Koressaar T, Remm M. Enhancements and modifications of primer design program Primer3. Bioinformatics 2007;23:1289–1291. doi: 10.1093/bioinformatics/btm091

42. Untergasser A, Cutcutache I, Koressaar T, Ye J, Faircloth BC, Remm M, Rozen SG. Primer3--new capabilities and interfaces. Nucleic Acids Res 2012;40:e115. doi: 10.1093/nar/gks596

43. Livak KJ, Schmittgen TD. Analysis of relative gene expression data using real-time quantitative PCR and the $2^{-\Delta\Delta C_T}$ method. Methods 2001;25:402-8. doi: 10.1006/meth.2001.1262

44. Sambrook JF, Fritsch EF, Maniatis T. Molecular Cloning - A Laboratory Manual. 3rd ed. New York: Cold Spring Harb Lab Press; 1989. ISBN 978-1-936113-41-5

45. Tom R, Bisson L, Durocher Y. Transfection of adherent HEK293-EBNA1 cells in a six-well plate with branched PEI for production of recombinant proteins. CSH Protoc 2008;2008:pdb.prot4978. doi: 10.1101/pdb.prot4978

46. Popović M, Žaja R, Fent K, Smital T. Molecular characterization of zebrafish Oatp1d1 (Slco1d1), a novel organic anion-transporting polypeptide. J Biol Chem 2013;288:33894-911. doi: 10.1074/jbc.M113.518506

47. Bradford MM. A rapid and sensitive method for the quantitation of microgram quantities of protein utilizing the principle of protein-dye binding. Anal Biochem 1976;72:248-54. doi: 10.1016/0003-2697(76)90527-3

48. Brzica H, Breljak D, Vrhovac I, Sabolić I. Role of microwave heating in antigen retrieval in cryosections of formalin-fixed tissues. In: Chandra U, editor. Microwave heating. Rijeka: IN-TECH Open; 2011. p. 41-62. doi: 10.5772/20319

49. Lee MG, Ohana E, Park HW, Yang D, Muallem S. Molecular mechanism of pancreatic and salivary gland fluid and HCO3⁻ secretion. Physiol Rev 2012;92:39-74. doi: 10.1152/physrev.00011.2011

50. Clark JS, Vandorpe DH, Chernova MN, Heneghan JF, Stewart AK, Alper SL. Species differences in Cl⁻ affinity and in electrogenicity of SLC26A6-mediated oxalate/Cl⁻ exchange correlate with the distinct human and mouse susceptibilities to nephrolithiasis. J Physiol 2008;586:1291-306. doi: 10.1113/jphysiol.2007.143222

303

Karaica D, et al. Sex-independent expression of Cfex (Slc26a6) in rat pancreas, small intestine, and liver, and male-dominant expression in kidneys
Arh Hig Rada Toksikol 2018;69:286-303

51. Garcia-Perez I, Villaseñor A, Wijeyesekera A, Posma JM, Stamler J, Aronson P, Unwin R, Barbas C, Elliott P, Nicholson J, Holmes E. Urinary metabolic phenotyping the slc26a6 (chloride-oxalate exchanger) null mouse model. J Proteome Res 2012;11:4425-35. doi: 10.1021/pr2012544

52. Jiang Z, Grichtchenko II, Boron WF, Aronson PS. Specificity of anion exchange mediated by mouse Slc26a6. J Biol Chem 2002;277:33963-7. doi: 10.1074/jbc.M202660200

53. Karniski LP, Lötscher M, Fucentese M, Hilfiker H, Biber J, Murer H. Immunolocalization of sat-1 sulfate/oxalate/bicarbonate anion exchanger in the rat kidney. Am J Physiol-Renal 1998;275:F79-87. doi: 10.1152/ajprenal.1998.275.1.F79

54. Costello JF, Smith M, Stolarski C, Sadovnic MJ. Extrarenal clearance of oxalate increases with progression of renal failure in the rat. J Am Soc Nephrol 1992;3:1098-104. PMID: 1482750

55. Hatch M, Freel RW, Vaziri ND. Intestinal excretion of oxalate in chronic renal failure. J Am Soc Nephrol 1994;5:1339-43. PMID: 7893999

56. Green ML, Hatch M, Freel RW. Ethylene glycol induces hyperoxaluria without metabolic acidosis in rats. Am J Physiol-Renal 2005;289:F536-43. doi: 10.1152/ajprenal.00025.2005

57. Iguchi M, Takamura C, Umekawa T, Kurita T, Kohri K. Inhibitory effects of female sex hormones on urinary stone formation in rats. Kidney Int 1999;56:479-85. doi: 10.1046/j.1523-1755.1999.00586.x

58. Lee YH, Huang WC, Huang JK, Chang LS. Testosterone enhances whereas estrogen inhibits calcium oxalate stone formation in ethylene glycol treated rats. J Urology 1996;156:502-5. PMID: 8683725

59. Farinelli MP, Richardson KE. Oxalate synthesis from [$^{14}C_1$] glycollate and [$^{14}C_1$]glycoxylate in the hepatectomized rat. Biochim Biophys Acta 1983;757:8-14. doi: 10.1016/0304-4165(83)90146-0

60. Meier PJ, Valantinas J, Hugentobler G, Rahm I. Bicarbonate/sulfate (electroneutral), bicarbonate/oxalate or sulfate/oxalate exchange in canalicular rat liver plasma mebrane vesicles. Am J Physiol-Gastr L 1987;253:G461-8. doi: 10.1152/ajpgi.1987.253.4.G461

61. Boyer JL. Bile formation and secretion. Compr Physiol 2013;3:1035-78. doi: 10.1002/cphy.c120027

62. Sugimoto T, Osswald H, Yamamoto K, Kanazawa T, Iimori H, Funae Y, Kamokawa S, Kishimoto T. Fate of circulating oxalate in rats. Eur Urol 1993;23:485-9. doi: 10.1159/000474659

Spolno-neovisna ekspresija izmjenjivača klora i mravlje kiseline Cfex (Slc26a6) u gušterači, tankom crijevu i jetri štakora i povišena ekspresija u bubrezima mužjaka

Izmjenjivač klora i mravlje kiseline (CFEX; SLC26A6) posreduje prijenos oksalata u različitim organima sisavaca. Pokusi u miševa s isključenim genom *Cfex* upućuju na moguću ulogu toga prijenosnika u razvoju hiperoksalurije i oksalatne urolitijaze, češćih u muških osoba. Štakori su važan model za istraživanje toga patofiziološkoga stanja, ali su spoznaje o lokalizaciji i regulaciji Cfex-a (rCfex) u njihovim organima nedostatne. U ovom radu primijenili smo metode RT-PCR i imunokemije u svrhu istraživanja ekspresije *rCfex* mRNA i proteina te regulacije istih spolnim hormonima u gušterači, tankom crijevu, jetri i bubrezima u različito tretiranih odraslih i predpubertetskih štakora obaju spolova. *rCfex* cDNA-transficirane stanice HEK293 uporabljene su za potvrdu specifičnosti komercijalnoga protutijela. Različiti biokemijski parametri izmjereni su u 24-satnom urinu, prikupljenom u metaboličkim kavezima. Ekspresija *rCfex* mRNA i proteina bila je prisutna u svim ispitanim organima. O spolu neovisna ekspresija prijenosnika rCfex nađena je u apikalnoj domeni interkaliranih kanalića gušterače, četkastoj membrani enterocita u tankom crijevu (duodenum > jejunum > ileum) i kanalikularnoj membrani hepatocita. U bubrezima je a) prijenosnik rCfex imunolokaliziran u četkastoj membrani proksimalnih kanalića sa segment-specifičnim obrascem (S1=S2<S3) i b) ekspresija *rCfex* mRNA i proteina iskazala je spolne razlike (mužjaci > ženke) zbog stimulacijskoga učinka androgena nakon puberteta. Međutim, izlučivanje oksalata urinom nije bilo sukladno ekspresiji bubrežnoga prijenosnika rCfex. Dakle, nejasan je učinak povišene ekspresije prijenosnika rCfex u proksimalnim kanalićima mužjaka na izlučivanje oksalata, a postojanje prijenosnika u kanalikularnoj membrani hepatocita mogući je put izlučivanja oksalata putem žuči.

KLJUČNE RIJEČI: *anionski izmjenjivač; bubrežni kamenci; imunolokalizacija; oksalurija; RT-PCR; spolne razlike; urolitijaza*